Measurement of AC conductance, and minima in loss tangent, of random conductor-insulator mixtures

1993 J. Phys.: Condens. Matter 5 2377

(http://iopscience.iop.org/0953-8984/5/15/009)

J. Phys.: Condens. Matter 5 (1993) 2377–2388. Printed in the UK

Measurement of AC conductance, and minima in loss tangent, of random conductor–insulator mixtures

R K Chakrabarty, K K Bardhan and A Basu
Saha Institute of Nuclear Physics, Sector-1, Block-AF, Bidhannagar, Calcutta-700 064, India

Received 14 August 1992, in final form 30 November 1992

Abstract. The complex AC conductance of carbon–wax mixtures was measured as a function of angular frequency ω from 7 Hz to 100 kHz for different concentrations p of carbon near the percolation threshold p_c. The scaling exponents, $x = 0.72 \pm 0.01$, $y = 0.23 \pm 0.05$ were found to be remarkably close to the theoretical values expected from the intercluster polarization model. The characteristic frequency ω_c at which the real part of the AC conductance deviates from its DC value scales with the DC conductance σ_{DC} as $\omega_c \sim \sigma_{DC}^z$, where $z \approx 1.1$. The nature of the variation of loss tangent $\tan\delta$ with frequency was studied in detail. It was found that $\tan\delta$ went through a minimum at a frequency which increased with p. The increase of $\tan\delta$ at higher frequencies cannot be explained by the usual RC model. We consider a modified version, the R–RC model in which a capacitor is always in series combination with a resistor, i.e. capacitors are lossy. This model is shown to reproduce the observed behaviour of $\tan\delta$ and believed to be more realistic than the RC model hitherto considered in that series resistors may be a more effective representation of the dangling bonds in the system.

1. Introduction

Much effort, both theoretical and experimental, has been made to understand the AC response of random binary mixtures of conductors and insulators [1]. As expected, the AC response is richer and more varied than the static one. The AC response could be either linear [1] or non-linear [2]. Here we restrict ourselves to consideration of only the linear response, i.e. to cases where the strength of the applied signal is sufficiently small. Such random mixtures have been successfully modelled as a percolating system where the conductors occur with probability p and the insulators with probability $1 - p$. Such systems undergo a metal–insulator transition at a critical concentration p_c of the conductors, known as the percolation threshold [3]. As one approaches the critical concentration p_c from the conducting side of the transition ($p > p_c$), the DC conductivity $\Sigma(p, 0)$ vanishes as $\Sigma(p, 0) \sim (p - p_c)^t$, whereas upon approaching p_c from above or below, the DC dielectric constant $\epsilon(p, 0)$ diverges as $\epsilon(p, 0) \sim |p_c - p|^{-s}$ [3].

The linear AC response in such a system is conveniently discussed by considering the scaling form of the complex AC conductance Σ of the network [1, 4–10]:

$$\Sigma(p, \omega) \sim |\Delta p|^t g_{\pm}\left(\frac{j\omega}{\omega_c}\right) \tag{1}$$

where $j = \sqrt{-1}$, ω is the applied frequency and ω_c is a characteristic frequency scale given by

$$\omega_c = \omega_0 |\Delta p|^{s+t} \sim \sigma_{DC}^z \tag{2}$$

0953-8984/93/152377+12$07.50

where σ_{DC} is the DC conductance and $z = (s+t)/t$. ω_0 is a microscopic frequency scale. If the conductivity of conductors is σ_0 and the dielectric constant of insulators is ϵ_0, then ω_0 is given by $\sigma_0/4\pi\epsilon_0$. g_+ and g_- are two different scaling functions for p above, and below, p_c respectively. At $p = p_c$, equation (1) reduces to

$$\Sigma(p_c, \omega) \sim \left(\frac{j\omega}{\omega_c}\right)^x \tag{3}$$

where $x = t/(s+t)$. If we define $\sigma \equiv \mathrm{Re}\,\Sigma(p,\omega)$ and $\epsilon \equiv \mathrm{Im}\,\Sigma(p,\omega)/\omega$, then according to (3)

$$\sigma(p_c, \omega) \sim \omega^x \qquad \epsilon(p_c, \omega) \sim \omega^{-y} \tag{4}$$

where $y = s/(s+t)$. It is easily seen that the critical exponents x and y satisfy the following hyperscaling relation

$$x + y = 1. \tag{5}$$

Equation (5) is, in fact, a consequence of more general arguments [5]. For $p > p_c$ it is seen from (1) that the characteristic frequency, ω_c separates two frequency regimes such that for $\omega < \omega_c$, $\sigma(p,\omega) \approx \sigma(p,0)$ and for $\omega_c < \omega < \omega_0$ the scaling relation (4) for σ holds. For $p < p_c$ similar results apply for $\epsilon(p,\omega)$. Two different physical processes have been suggested to explain the AC response of a random binary mixture, namely intercluster polarization effects (ICP) [1,4–10] and (2) anomalous diffusion within clusters (AD) [11]. The expressions for the various exponents shown above are actually applicable to models based on ICP only. The predictions of the model [11] based on AD are qualitatively the same but the individual expressions of the critical exponents are different, e.g. $\omega_c \sim \Delta p^{\nu(2+\theta)}$, where $\theta = (t - \beta/\nu)$, β and ν being the exponents for the mass of the backbone and correlation length respectively. The exponents x and y are given by $x = t/\nu(2+\theta)$, $y = (2\nu - \beta)/\nu(2+\theta)$. In the lattice model incorporating ICP, also known as the RC model [1,4–10], occupied bonds are considered as pure resistors of resistance R_0 occuring with probability p, the conductor fraction. Unoccupied bonds are considered as perfect capacitors of capacitance C_0 occuring with the probability $1-p$. The microscopic frequency scale in this case is given by $\omega_0 = 1/R_0C_0$.

On the experimental side, Laibowitz and Gefen [12] measured the AC conductivity and dielectric constant for thin Au films of varying thickness near p_c, from 100 Hz to 10M Hz. They found that $x = 0.95 \pm 0.05$ and $y = 0.13 \pm 0.05$. These values are in agreement with the hyperscaling relation (5), but are individually different from the predictions either for $d = 2$ ($x = y = 0.5$ in ICP based models or $x = 0.33$, $y = 0.67$ in the AD model) or for $d = 3$ ($x = 0.72$, $y = 0.28$ in ICP based models or $x = 0.58$, $y = 0.42$ in the AD model). Song *et al* [13] measured the exponents x and y in carbon–teflon mixtures to be $x = 0.86 \pm 0.06$ and $y = 0.12 \pm 0.04$. These values are closer to the predictions of ICP based models than those of the AD model in $d = 3$. Interestingly, their values are also close to those found by Laibowitz and Gefen [12] but still higher than the theoretical values. In both of these experiments, it was found out that both the AC resistance $R(p,\omega) \sim 1/\sigma(p,\omega)$ and the AC capacitance $C(p,\omega) \sim \epsilon(p,\omega)$ followed a single power law in the critical region. However Hundley and Zettl [14] reported that there were two power law regimes in R–ω as well as for the C–ω curve although the general scaling relation (5) was still obeyed in both the regions. They also plotted the characteristic frequency as a function of the DC

resistance and found z to be equal to 0.82. However this value of z is not compatible with the predictions of either of the two models ($z = 2$ and 1.4 (ICP based models) and 3 and 1.4 (AD model) in 2D and 3D respectively). The paucity of data may be a possible source this discrepancy. Yoon and Lee [15] measured the AC conductivity and dielectric constant of two-dimensional lattice percolation systems, generated artificially on an Al film. The measured values of $x = 0.995 \pm 0.05$ and $y = 0.024 \pm 0.005$ are not in agreement with either of the two models although relation (5) still holds good.

The French group [1, 16–19] pointed out that the loss tangent $\tan\delta$, defined as the ratio of the real and imaginary parts of the complex conductivity, had some interesting properties. For example, at $p = p_c$, (1) yields an universal loss angle given by

$$\delta_c \equiv \delta(p_c, \omega) = (\pi/2)(1 - x). \tag{6}$$

δ_c depends only on the dimensionality, while δ is a function of p and ω. When p is differs slightly from p_c it is expected that the universal value of $\tan\delta_c$ will still be observed in the frequency range, $\omega_c \ll \omega \ll \omega_0$. At low frequencies the loss tangent depends crucially on the sign of Δp. For $p > p_c$,

$$\tan\delta \sim |\Delta p|^{s+t}/\omega \qquad \omega \ll \omega_c \tag{7a}$$

$$\tan\delta = \tan\delta_c \qquad \omega_c \ll \omega \ll \omega_0. \tag{7b}$$

For $p < p_c$,

$$\tan\delta \sim \omega/|\Delta p|^{s+t} \qquad \omega \ll \omega_c \tag{8a}$$

$$\tan\delta = \tan\delta_c \qquad \omega_c \ll \omega \ll \omega_0 \tag{8b}$$

Experimental data on loss angle are rather scant. Laugier *et al* [20] working with random mixtures of plain and silver-coated glass microbeads measured $\tan\delta(\omega)$ as a function of frequency for $p < p_c$ and found a minimum. The value of the minimum, 0.55 ± 0.05, was compared with the value of 0.47 ± 0.04 expected from (6). The authors also noted that the rise of the loss tangent for $p < p_c$ in the low-frequency side of the minimum was unexpected. Van Dijk *et al* [21] working with a very different system of microemulsions found $x = 0.62 \pm 0.02$ from the plot of $\tan\delta$ versus frequency.

In this paper, we present the results of our measurements of linear AC response of three-dimensional mixtures of carbon and wax near the percolation threshold. We determined the values of the exponents x and y to be 0.72 ± 0.01 and 0.23 ± 0.05 which are remarkably close to their theoretical values in the ICP model. However, the value of z, which is theoretically just the inverse of x, is found to be 1.1 ± 0.1. The latter is somewhat smaller than the theoretical value of 1.4. However our main focus is on the frequency regime where the loss tangent $\tan\delta$ assumes a minimum value, $\tan\delta_m$. It is found in particular that $\tan\delta_m$ is a function of σ_{DC} (i.e. p) and appears to have a value ~ 0.52 in the limit σ_{DC} approaching zero (i.e. p approaching p_c). This value compares quite well with the universal value of the loss tangent in three dimensions, 0.47. The behaviour of $\tan\delta(p, \omega)$ near the minimum, particularly on the higher frequency side is the opposite to that given by the 'effective medium approximation' (EMA) treatment of the usual RC model. We propose a modification of the above model that seems to generate the desired behaviour in $\tan\delta$. The modified model or R–RC model is obtained from the RC model by replacing each capacitor with a series combination of a resistor and a capacitor. In effect, a perfect capacitor is being

replaced with a lossy one. Carbon–wax samples have previously been used for studying applications such as switching devices [22], $1/f$ noise [23], the dielectric constant [24], non-linear I–V characteristics [25] and non-linear AC response [2]. AC measurements have been also performed on other systems like Ag–KCl mixtures [26, 27] and porous ceramic [28]. The advantage of using carbon in a percolating system has been noted previously [13, 25]. Below we present experimental details in section 2, results in section 3, discussion in section 4 and conclusion in section 5.

2. Experimental details

We used carbon as the conducting and paraffin wax as the insulating component. The sample preparation procedure is the same as reported in [25]. Samples used in AC measurements have their nominal p values between 0.6% and 1%, i.e. very close to $p_c \sim 0.76\%$ by volume of carbon. It may be noted that the value of p_c is much lower than the theoretical value of 15%. Near p_c, the fluctuation in DC resistances of samples in a given batch (i.e. corresponding to same nominal p) may be large as shown in [25]. Thus R_{DC}, rather than p, is used to characterize samples with $p > p_c$ [25, 12]. The DC conductivity exponent, t, was found to be 2.1 in agreement with the theoretical value. The samples are in the form of circular discs 1 cm in diameter and 2 mm in thickness. During measurements, samples were held between two brass electrodes, having diameters slightly larger than the diameter of the samples. The two-probe method was used for the measurement of impedances as the contact resistance is small compared to the sample resistances. All measurements were carried out when sample resistances attained steady values [25]. The magnitude and phase angle of the complex conductance Σ were measured as a function of frequency from 7 Hz to 100 kHz, using a model 124A lock-in amplifier (LIA). As the input impedance of the LIA is much smaller than the impedances of the samples, an attenuator circuit having a very large input impedance and very small output impedance was used. The circuit also served as a current-to-voltage converter. The sample was placed at the input of the circuit. In order to eliminate any error in the phase measurement, at each frequency the phase-sensitive detection was made first with a standard carbon resistor and then with the sample. The difference in the two readings represented the extra phase introduced in the signal due to the sample. The amplitude of the input signal was kept at a low value (typically 10–20 mV) in order to avoid any voltage-induced non-linear effect [2, 25]. The DC output from the LIA was fed into a digital voltmeter that was interfaced with a personal computer. The data were averaged and processed in a personal computer. From the magnitude $|\Sigma|$ and phase θ of the complex conductance Σ, the AC conductance $\sigma = |\Sigma| \cos\theta$, capacitance $C = |\Sigma| \sin\theta/\omega$, and loss angle $\delta = \pi/2 - \theta$ were found. Measurement errors were usually small, being less than the symbol size in the figures. However fluctuation in some derived quantities (e.g. ω_c or δ_m) could be large because of sample-to-sample variation.

3. Results

Figure 1 shows the variation of AC conductance σ with frequency ω in log–log scale for five different samples having their DC resistance R_{DC} between 60 kΩ and 20 MΩ. These samples have their nominal p values very close to p_c. Curves belonging to different R_{DC} clearly demonstrate the consistency in characterizing samples by R_{DC}. These conform to the behaviour discussed previously and also as reported by Laibowitz and Gefen [12] and

Song *et al* [13]. At low frequency, $\sigma(p,\omega)$ differs little from its DC value, σ_{DC}. At high frequency $\sigma(p,\omega)$ scales with ω according to (4) and as indicated by a straight line in figure 1. The characteristic frequency, ω_c and the exponent x were found from the scaled data as shown in figure 2. We note from (1) that the scaling functions, g_+ and g_- depend only on ω/ω_c. Accordingly, the reduced AC conductivity $\sigma_{sc} = \sigma(p,\omega)/\sigma(p,0)$ were plotted against reduced frequency $\omega_{sc} = \omega/\omega_c$ for seven different samples with DC resistance values between 2 MΩ and 20 MΩ, i.e. for p very close to p_c. It is seen that data belonging to different σ_{DC} (i.e. different p) do indeed collapse into a single curve. In obtaining the scaled plot, $\sigma_{DC} = \sigma(p,0)$ and ω_c were treated as fitting parameters and were adjusted to obtain the best fit. In the region $\omega_{sc} \gg 1$, σ_{sc} was fitted to ω_{sc} with a power law $\sigma_{sc} \sim \omega_{sc}^x$ (4) which yields $x = 0.72 \pm .01$. ω_c decreases with σ_{DC}. Figure 3 shows a log–log plot of σ_{DC} and ω_c for different samples. A least-square fit according to the power law $\omega_c \sim \sigma_{DC}^z$ (2) gives $z = 1.1 \pm 0.1$. The value of the exponent x is practically the same as the theoretical value in the ICP model [1]. It is to be noted that the value found by Song *et al* [13] who also used carbon, but with teflon, was higher than the present one. We ascribe the discrepancy in z between the the present work and the theoretical value to the inadequate range of data as clearly seen in figure 3. Both σ_{DC} and ω_c cover little more than a decade of values. The value of $z \sim 0.8$ reported by Hundley *et al* [14] is even less than the present one and it is possible that in this case also an inadequate range of data could be the cause. Note that Au films that were used as samples were more likely to be three-dimensional rather than two-dimensional in nature [29].

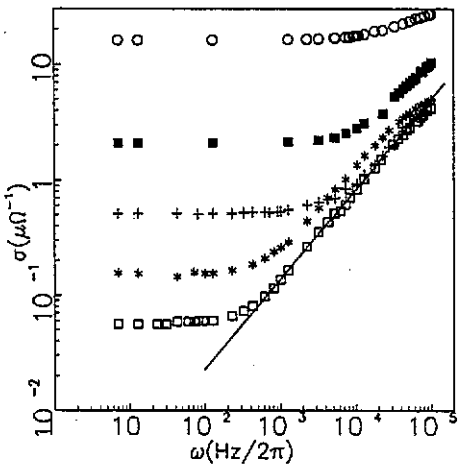

Figure 1. A plot of the real part of AC conductance Σ versus angular frequency for five different samples with $p > p_c$. The straight line indicates a typical scaling region.

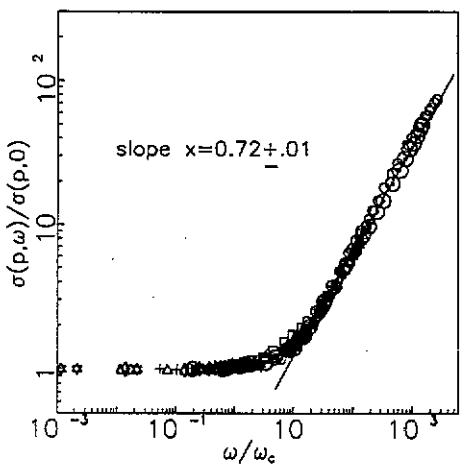

Figure 2. A plot of the scaled AC conductance $\Sigma(p,\omega)/\Sigma(p,0)$ versus scaled frequency ω/ω_c. The straight line is a power-law fit to the scaled data in the high-frequency regime with the value of the slope as indicated.

The variation of AC capacitance $C(\omega)$ of four different samples, all having $p < p_c$ as a function of freqency, ω is shown in figure 4. Similar to the case of $\sigma(\omega)$, $C(\omega)$ remains constant for small ω, but for large ω, data were fitted to the power law $C(\omega) \sim \omega^{-y}$ according to (4) (capacitance being proportional to dielectric constant). The value obtained was $y = 0.23 \pm 0.05$. It should be noted that capacitance data are more error-prone than

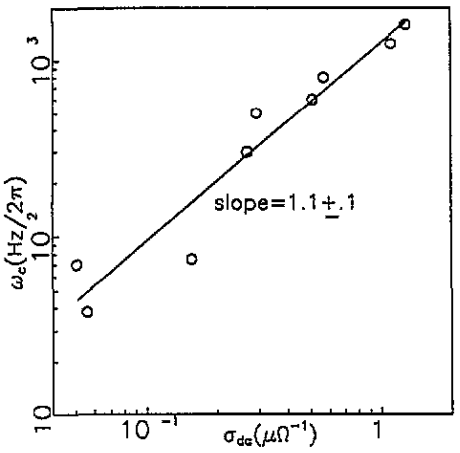

Figure 3. A plot of characteristic frequency ω_c versus DC conductance σ_{DC} in $\mu\Omega^{-1}$ on a log–log scale. The straight line is a power-law fit to the data with the value of the slope as indicated.

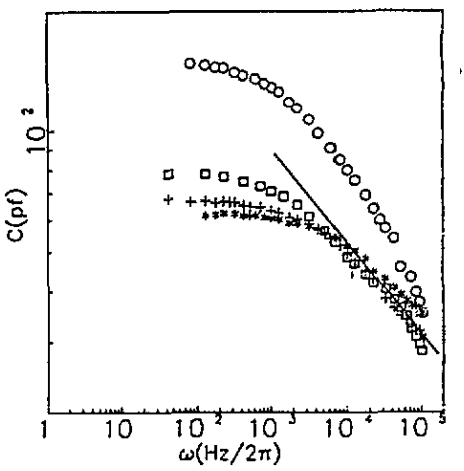

Figure 4. A plot of AC capacitance C versus angular frequency ω in four different samples having $p < p_c$. The straight line has a slope of 0.23 which is an average of the exponents found from power-law fit to the data.

conductance data. This, along with the limited range of data, makes the value of y much less reliable than that of x [12, 13]. Nevertheless the two exponents are compatible with the hyperscaling relation (5).

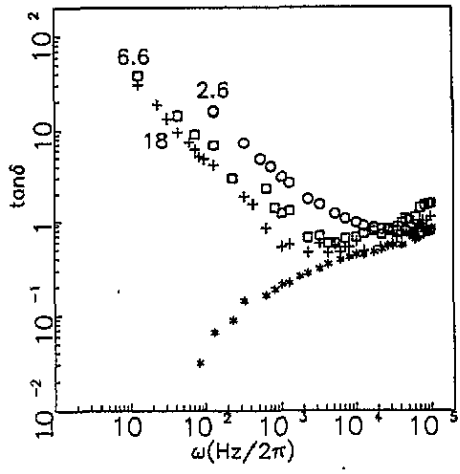

Figure 5. A plot of loss tangent $\tan\delta$ versus angular frequency ω for four different samples. The DC resistances of three samples in MΩ with $p > p_c$ are indicated on the respective curves. The remaining curve (*) corresponds to a sample with $p < p_c$.

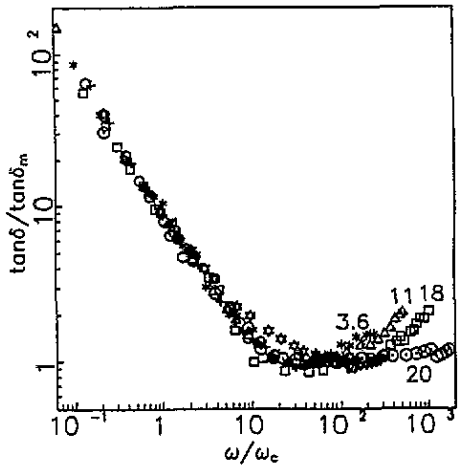

Figure 6. A plot of scaled loss tangent $\tan\delta/\tan\delta_m$ versus scaled frequency ω/ω_c for six different samples. The DC resistances in MΩ of some of the data are indicated on the curves.

Figure 5 shows the variation of loss tangent $\tan\delta$ with frequency for different DC resistances and hence for different p. For clarity only a few typical curves have been shown. For $p > p_c$ the value of R_{DC} is marked on each curve. The curve (*) shows the typical behaviour for $p < p_c$. Note that the loss angle, δ is related to the phase, θ

as $\delta = \pi/2 - \theta$. At low ω, for $p > p_c$, $\tan\delta$ is large and decreases with ω whereas for $p < p_c$, $\tan\delta$ is very small and increases with ω. Such a difference in behaviour illustrates the sensitive nature of the dependence of $\tan\delta$ on the sign of Δp in accordance with (7) and (8). The following salient features of the behaviour of the loss tangent for $p > p_c$ as a function of applied frequency in the carbon–wax system are evident in the curves in figure 5:

(i) $\tan\delta \equiv \tan\delta(p, \omega)$ is a concave function of ω. At low ω, $\tan\delta$ decreases with increasing ω. For samples of sufficiently large DC resistances, as ω increases to ω_m, it reaches a minimum value, $\tan\delta_m$, and then, bends upward to higher value with small,varying slopes. $\tan\delta$ is asymmetric about its minimum. ω_m decreases with increasing R_{DC}. Within the frequency range used in this work ($\leqslant$ 100 kHz), only samples with $R_{DC} \geqslant 2$ MΩ are found to have minima in $\tan\delta$ at high frequencies. Samples with $R_{DC} < 2$ MΩ possibly may have minima in $\tan\delta$ at still higher frequencies. Thus the system as a function of ω starts out being dissipative in nature, then becomes increasingly capacitive and again tends to become more dissipative. It is interesting to note that the increase of $\tan\delta$ at high frequencies has been also observed in mixtures of conducting and non-conducting glass beads [20]. It seems likely that such behaviour will be rather common in other similar systems.

(ii) Although curves for different R_{DC} at low frequencies are quite spaced apart those at high frequencies, including the one for $p < p_c$, are seen to become bunched.

(iii) $\tan\delta_m \equiv \tan\delta_m(p)$ is a decreasing function of R_{DC}.

Keeping in mind especially the last two features above, we present a log–log plot of the reduced loss tangent, $\tan\delta/\tan\delta_m$, versus the reduced frequency, ω/ω_c, in figure 6 for seven different samples with $p > p_c$. Values of R_{DC} in MΩ are marked on some of the curves. As before, $\tan\delta_m$ and ω_c were adjusted to get the best fit. It may be noted that the ω_c for a given sample thus found is in general somewhat different from that found earlier from the scaled conductance data in figure 2. In figure 6 it is seen that the different set of data points collapses into a single curve for small ω_{sc} but fail to do so for large ω_{sc}. This is perhaps not unexpected because the scaling relation (1) is not valid for $\omega > \omega_0$. In the region $\omega_{sc} < 10$, the data are linear with a slope ≈ -0.9 as expected from (7*a*). Figure 7 shows a plot of $\delta_m(p)$ versus $\sigma^{1/t}$ in linear scale, showing clearly the variation of the loss-tangent minima with sample DC conductances. The reason for such choice of the plot variables will be discussed later. The scatter in the data, however, does not permit any firm conclusion to be drawn about the nature of the variation. Assuming a linear relation the least-square fit yields for the intercept a value of 0.48 rad, corresponding to $\tan\delta(p_c) \approx 0.52$. The corresponding value expected from (6) in 3D is 0.47. The limit of $\tan\delta(p)$ corresponds to $x = 0.69$. The latter compares very well with the value determined earlier from the scaled conductance data in figure 2.

4. Discussion

Experiments have generally confirmed that inter-cluster polarization effects provide a physical framework in understanding time-varying electrical properties of random binary mixtures of conductors and insulators, of which the carbon–wax mixture is a particular example. Within ICP-based models such a mixture is considered as a network of resistors (fraction, p) and capacitors (fraction, $1 - p$) representing the polarizability of the insulating medium. Song *et al* [13], using this picture has given a qualitative description of results

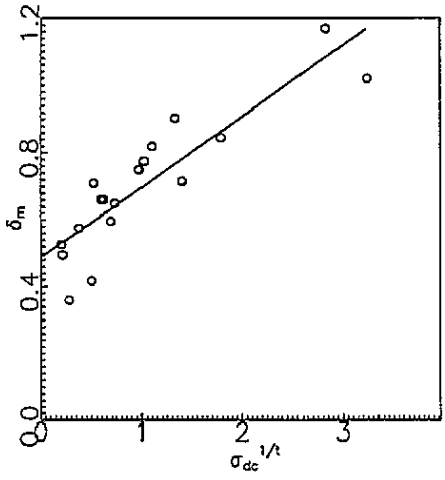

Figure 7. A plot of the minimum value of loss angle δ_m versus $\sigma_{DC}^{1/t}$ where σ_{DC} is the DC conductance of the sample and t is the static conductivity exponent. The straight line is a least-square fit to the data.

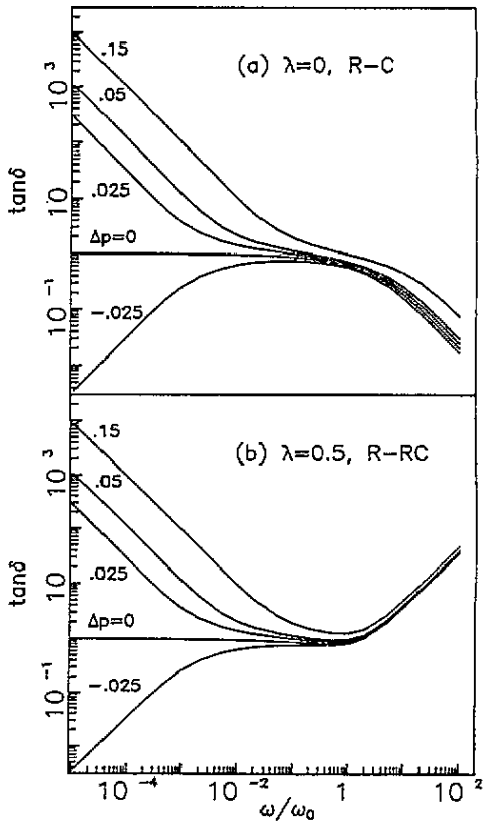

Figure 8. A plot of $\tan\delta$ versus ω/ω_0 as calculated from (*a*) *RC* model (*b*) *R–RC* model using EMA. The values of Δp are indicated on the curves. See text for discussion of the model parameter λ.

such as displayed in curves in figures 1, 4 and 5. For $p > p_c$ and under a low-frequency AC field, the current through a sample is entirely carried by the backbone consisting of resistors, as the capacitive junctions constitute very high-impedance paths. Consequently AC conductance differs little from its DC value and the phase θ is small. As ω increases, the impedance of the capacitive junctions decreases and as a result the current finds more parallel paths to flow along. Therefore $|\Sigma|$ and θ increase. This is consistent with the fact that $\sigma(\omega)$ increases and $\tan\delta(\omega)$ decreases with increasing ω. For a sample with smaller p (i.e. closer to, but still above, p_c) there will be fewer channels for the current to flow along. This makes capacitive paths comparable to resistive ones at frequencies lower than before. Consequently ω_c will be lower. For $p < p_c$, capacitive junctions will be predominant as there is no connected path through conductors. Thus the phase (loss angle) will be close to 90°.

4.1. EMA and scaling results: RC model

Let us now discuss concrete predictions based on the above physical framework. The scaling theory (1) has already been introduced and its predictions compared to our data in the result section. The scaling theory, as we found out, is most appropriate to account

for critical properties near p_c. Results concerning various exponents give evidence to this. However it is known that the EMA treatment [1, 10, 30] is capable of producing a qualitatively correct, global picture. While some of its predictions (e.g. the value of exponents in critical regions) are quantitatively incorrect, they are useful nevertheless in obtaining information that is difficult to obtain otherwise. The EMA predictions on the behaviour of the real and imaginary parts of the AC conductance have been discussed in detail by many workers [1, 10]. For example, values of both s and t are found to be equal to 1. We now discuss the predictions of the EMA on the behaviour of $\tan\delta$ as a function of ω. For later convenience, let us first consider a more general model in which the lattice consists of bonds having two conductances, σ_1 (fraction p) and σ_2 (fraction $1-p$). Two bond conductances can themselves be arbitrary complex admittances. Clearly, the RC model is a particular example with

$$\sigma_1 = 1/R \qquad \sigma_2 = j\omega C. \tag{9}$$

Thus in the RC model one type of conductors is purely resistive and another type purely capacitive. The EMA formula for the complex conductance is given by

$$\Sigma = [\sigma_1/2(d-1)][d\Delta p + (d-2-d\Delta p)h + \Delta] \tag{10a}$$

with

$$\Delta = [d^2\Delta p^2 + (d-2-d\Delta p)^2h^2 + 2(2(d-1) + (d-2)\Delta p - d^2\Delta p^2)h^2]^{1/2} \tag{10b}$$

$$h = \sigma_2/\sigma_1. \tag{10c}$$

d is the dimensionality and $\Delta p = p - 1/d$ since $1/d$ is the percolation threshold in the EMA treatment. In the RC model (9) and (10c) give $h = j\omega/\omega_0$, $\omega_0 = 1/RC$. Figure 8(a) shows a log–log plot of $\tan\delta$ against the reduced frequency ω/ω_0 obtained numerically from equations (10) in the RC model in three dimensions (see also figure 29 in [1]). It is easily verified that at low frequencies, $\omega < \omega_0|\Delta p|^2$,

$$\tan\delta \sim |\Delta p|^2/\omega \qquad p > p_c \tag{11a}$$

$$\tan\delta \sim \omega/|\Delta p|^2 \qquad p < p_c. \tag{11b}$$

At high frequencies, $\omega > \omega_0$ and for p above or below p_c, we have

$$\tan\delta \sim (4 + O(\Delta p))/\omega \qquad d = 3. \tag{12}$$

Thus we see that in the RC model $\tan\delta(p > p_c)$ is a decreasing function of ω at both low and high limits in three dimensions. However, this is in contradiction with our observation (i). This EMA result has also been confirmed by using the transfer matrix algorithm [17]. For $\omega > \omega_0$, dielectric bonds are much better conductors than the metallic ones. Since $p_c < \frac{1}{2}$ for a cubic lattice, the dielectrics percolate for $p < p_c$. Thus, with increasing frequency, the dielectric bonds will carry relatively more currents than the conducting bonds. Therefore, $\tan\delta$ should decrease with increasing ω. Since, in our samples $p_c = 0.76\%$ by volume the same nature of variation of $\tan\delta$ is expected. Notice that the high-frequency behaviour as given by (12) in the EMA treatment is not available from the scaling theory. The low-ω behaviour agrees with that in (7) and (8) obtained from scaling theory with ($s = t = 1$) and also with the data in figure 6. Furthermore, according to (11), at low frequencies $\tan\delta$ is

(inversely) proportional to $|\Delta p|^2$ for p (less) greater than p_c whereas at high frequencies $\tan\delta$ is, to the first approximation, independent of $|\Delta p|$. This explains observation (ii).

The curves in figure 8(a) are seen to exhibit minima though they are quite broad. This is more transparent in the scaling relation (3) which implies that $\tan\delta$ remains constant in the frequency range $\omega_c < \omega < \omega_0$, where the constant value of δ is given by (6). As shown in figure 5, δ_m, the minimum value δ depends on p and is larger for smaller R_{DC} (observation (iii)). This is also in agreement with the numerical data in figure 8(a). To obtain a more quantitative result, we again turn to the scaling relation (1). At $p \approx p_c$, and $\omega \ll \omega_0$ it can be shown that to first order in Δp, $\Sigma(p,\omega) \approx \Sigma(p_c,\omega)(1 + aj^{-1/(s+t)}\Delta p)$. a is a small constant. The second term within the bracket gives rise to the scaling correction which gives

$$\delta_m \equiv \delta(\omega \ll \omega_0) \approx \delta_c + a \sin[\pi/2(s+t)]\Delta p. \tag{13}$$

Thus $\delta_m - \delta_c$ should be proportional to Δp, i.e. to $\sigma_{DC}^{1/t}$. This provides the motivation for choosing the variables in figure 7.

4.2. *EMA and scaling results: the R–RC model*

From the previous discussion we see that while the RC model can explain certain features, e.g. observations (ii) and (iii) as well as the low-frequency behaviour of $\tan\delta$, it predicts quite the opposite behaviour at high frequencies (figure 8(a)). The present system of carbon and wax becomes more dissipative while the RC model predicts a more capacitive system. It seems probable that the assumption of perfect capacitors in the RC model is not very realistic in the sense that in real samples there will always be conductors in the form of dangling bonds separating insulating regions. In other words, the possibility of conduction solely through capacitors does not exist. The dangling bonds are resistive in nature but irrelevant in consideration of the backbone's conduction properties. However they should play an important role in the consideration of intercluster effects. We have tried to reinforce the effects of these bonds by adding a resistance in series with each capacitor in the RC model. At very high frequencies the capacitors will behave almost like zero-impedance conductors in the presence of series resistors which will then determine the overall electrical behaviour of the network.

In the R–RC model, we have

$$\sigma_1 = 1/R \qquad \sigma_2 = j\omega C/(1 + j\omega CR') \tag{14}$$

Compare (14) with (9). Here R' is the resistance in series with capacitance C. From (10c) we have

$$h = (j\omega/\omega_0)/(1 + j\lambda\omega/\omega_0). \tag{15}$$

$\lambda = R'/R$ is the ratio of two resistive bond strengths. Alternatively, (15) could be written in terms of two frequency scales, ω_0 and $1/R'C$. It is seen that (15) reduces to the expression appropriate for the RC model as λ goes to 0, i.e., dangling bonds are neglected. Numerical data obtained by using (15) in (10) and for $\lambda = 0.5$ are shown in figure 8(b). Increasing the value of λ leaves the curves qualitatively unchanged. Upon decreasing the value of λ, the minima at $\tan\delta < 1$ will become increasingly pronounced. The data in figure 8(b), in contrast to those of figure 8(a), clearly display the desired features as described in observation (i). Features corresponding to observations (ii) or (iii) discussed previously

remain basically the same as in the *RC* model. The low-frequency behaviour is still described by (10). To consider the high-frequency behaviour, let us first note that the only complex variable in (10) is h. In the high-frequency limit, h approaches a real constant value equal to $1/\lambda$, i.e., the loss tangent tends to infinity as it does in the zero-frequency limit. In particular, equation (12) in the *RC* model changes to

$$\tan\delta \sim \omega \qquad d = 3 \tag{16}$$

in the *R–RC* model.

To find out the effect of (15) in the scaling formulation, we replace the factor $j\omega/\omega_0$ in (1) by right-hand side of (15) to obtain the following:

$$\Sigma(p,\omega) \sim |\Delta p|^t g_{\pm}\{[(j\omega/\omega_0)/(1 + j\lambda\omega/\omega_0)]|\Delta p|^{-s-t}\}. \tag{17}$$

The scaling relation (3) at $p = p_c$ will then become

$$\Sigma(p_c,\omega) \sim [(j\omega/\omega_0)/(1 + j\lambda\omega/\omega_0)]^x. \tag{18}$$

For equation (18) to hold, we must have $\omega/\omega_0 < 1/\sqrt{1-\lambda^2}$ and $\lambda \leqslant 1$. The scaling region in the *R–RC* model, unlike that in *RC* model, includes frequencies $\omega > \omega_0$. It is seen from (17) that the argument of the scaling function, in general, is no longer a function of ω/ω_c only. This does not affect the scaling property σ as shown in figure 1 as the dominant behaviour is given by the power law. However it does prevent the collapse of loss tangent data for different p at high frequencies as seen in figure 6. At low frequencies $\tan\delta$ is still a decreasing function of ω/ω_c only. The loss angle is given by

$$\delta(p = p_c) = \delta_c + (\pi\alpha u/2) \qquad \tan(\pi\alpha/2) = \lambda\omega/\omega_0. \tag{19}$$

In the *R–RC* model the loss angle at the percolation threshold is no longer a constant as in the *RC* model but a function of ω. Since it increases with ω, for $p > p_c$, a minimum will occur at a frequency $\omega_c < \omega < \omega_0\sqrt{1-\lambda^2}$. Since an explicit functional form of the scaling function g_+ is not known, it is not possible to obtain an analytic expression for δ_m. However δ_m of a very high-resistance sample should give an idea of the magnitude of the deviation from the universal constant. From the data in figure 5 and 7 we see that the factor α is indeed quite small. It is evident that δ_m is a function of p.

5. Conclusions

From the above discussion it is evident that we have largely succeeded in explaining much of our data within the *R–RC* model. ω_0 and λ are two constants of the model. However, it was not possible to relate any measured quantity directly to those parameters although there are ways to estimate orders of magnitude. For example, from frequencies where minima occur, it appears that ω_0 is of the order of a few kHz. However, this value is very small compared to the microscopic frequency scale of the system which is estimated to be of the order of 10^{15} Hz. It is not clear how to account for such a low value of ω_0. This problem was also noted earlier by Laugier *et al* [20]. It is interesting to note that a different variation of *RC* model, namely *RL–C* model, was used before to describe the optical properties of conductor–dielectric mixtures at high frequencies [1]. This indicates the possibility of describing various other frequency-dependent properties with an appropriate choice of bond conductances.

Acknowledgments

We thank A Chakrabarty, S Bose and R Ranganathan for their very useful suggestions and T K Pyne for technical help.

References

[1] Clerc J P, Giraud G, Laugier J M and Luck J M 1990 *Adv. Phys.* **39** 191 and the references therein
The symbol u in this review is the same as x in the present work
[2] Bardhan K K and Chakrabarty R K 1992 *Phys. Rev. Lett.* **69** 2559
[3] Stauffer D 1985 *Introduction to Percolation Theory* (London: Taylor and Francis)
[4] Efros A L and Shklovskii B I 1976 *Phys. Status Solidi* b **76** 475
[5] Bergman D J and Imry Y 1977 *Phys. Rev. Lett.* **39** 1222
[6] Straley J P 1977 *Phys. Rev.* B **15** 5733
[7] Stephen M J 1978 *Phys. Rev.* B **17** 4444
[8] Webman I 1981 *Phys. Rev. Lett.* **47** 1496
[9] Stroud D and Bergman D J 1982 *Phys. Rev.* B **25** 2061
[10] Wilkinson D, Langer J S and Sen P N 1983 *Phys. Rev.* B **28** 1081
[11] Gefen Y, Aharony A and Alexander S 1983 *Phys. Rev. Lett.* **50** 77
[12] Laibowitz R B and Gefen Y 1984 *Phys. Rev. Lett.* **53** 380
[13] Song Y, Noh T W, Lee S and Gaines J R 1986 *Phys. Rev.* **33** 904
[14] Hundley M F and Zettl A 1988 *Phys. Rev.* B **38** 10290
[15] Yoon C S and Lee S 1990 *Phys. Rev.* B **42** 4594
[16] Clerc J P, Tremblay A M S, Albinet G and Mitescu C D 1984 *J. Phys. Lett.* **45** L913
[17] Luck J M 1985 *J. Phys. A: Math. Gen.* **18** 2061
Clerc J P, Giraud G, Laugier J M and Luck J M 1985 *J. Phys. A: Math. Gen.* **18** 2565
[18] Laugier J M, Clerc J P, Giraud G and Luck J M 1986 *J. Phys. A: Math. Gen.* **19** 3153
[19] Laugier J M and Luck J M 1987 *J. Phys. A: Math. Gen.* **20** L885
[20] Laugier J M, Clerc J P and Giraud G 1986 *Proc. Int. AMSE Conf.,1986b* ed G Mesuard (Lyon: AMSE)
[21] Van Dijk M A 1985 *Phys. Rev. Lett.* **55** 1003
[22] Bueche F 1973 *J. Appl. Phys.* **44** 532
[23] Chen C C and Chou Y C 1985 *Phys. Rev. Lett.* **54** 2529
[24] Chou Y C and Jaw T S 1988 *Solid State Commun.* **67** 753
[25] Chakrabarty R K, Bardhan K K and Basu A 1991 *Phys. Rev.* B **44** 6771
[26] Grannan M, Garland J C and Tanner D B 1981 *Phys. Rev. Lett.* **46** 375
[27] Chen I and Johnson W B 1986 *J. Mat. Sci.* **21** 3162
[28] Brouers F and Ramsamugh A 1988 *J. Phys. C: Solid State Phys.* **21** 1839
[29] Coniglio A, Daoud M and Herrmann H J 1989 *J. Phys. A: Math. Gen.* **22** 4189
[30] Kirkpatrick S 1973 *Rev. Mod. Phys.* **45** 574; *Condensed Matter* vol III, ed R Balian, R Maynard and G Toulouse (Amsterdam: North-Holland)